C Gutiérrez-Montes, E Sanmiguel-Rojas, A Viedma, G Rein, Experimental Data and Numerical Modelling of 1.3 and 2.3 MW Fires in a 20 m Cubic Atrium Building and Environment 44, pp. 1827–1839, 2009.
doi:10.1016/j.buildenv.2008.12.010

Experimental Data and Numerical Modelling of 1.3 and 2.3 MW Fires in a 20 m Cubic Atrium

Cándido Gutiérrez-Montes [a,*], Enrique Sanmiguel-Rojas [a], Antonio Viedma [b], Guillermo Rein [c]

[a]Fluid Dynamics Division of the Department of Mining and Mechanical Engineering, University of Jaen, Jaen, Spain
[b]Department of Thermal and Fluid Engineering, Technical University of Cartagena, Murcia, Spain
[c]BRE Centre for Fire Safety Engineering, The University of Edinburgh, EH9 3JL, UK
[*]Corresponding author: Tel.: +34953212903; fax: +34953212870.
E-mail address: cgmontes@ujaen.es (C. Gutiérrez-Montes)
Postal address: Despacho 022/023, Área de Mecánica de Fluidos, Departamento de Ingeniería Mecánica y Minera, Edificio A3, Campus Las Lagunillas, 23009, Jaén, España.

Abstract:

Atria and large spaces are common architectonical features in modern buildings such as high rises, auditoria, warehouses, airports and mass transport stations among others. There is currently an international trend towards the performance-based design for fire safety of these building elements. This design process relies heavily on fire modelling but the knowledge in fire dynamics and the movement of smoke in atria and large spaces still presents some gaps. This paper aims at contributing to close these gaps and reports the three Murcia Atrium Fire Tests conducted in a 20 m cubic enclosure using pools of 1.3 and 2.3 MW. Detailed transient measurements of gas and wall temperatures, as well as pressure drop through the exhaust fans and airflow at the inlets were recorded. The study also includes the effect of the mechanical exhaust ventilation. Results have been compared with those predicted by the computational fluid dynamics (CFD) model Fire Dynamics Simulator FDSv4. In general terms, the comparisons between experiments and simulations show good agreement, especially in the far field of the plume, but the accuracy is poor at the lower plume region and near the flame.

Keywords:

Smoke, large enclosure, Murcia Atrium Fire Tests, CFD, FDS.

1.- Introduction:

An atrium within a building is a large open space created by an opening or a series of openings connecting two or more floors. This kind of structure has become a common feature in modern architecture and is commonly found in high rise buildings, auditoria, warehouses, airports and mass transport stations among others [1].

When a fire takes place in an atrium or a large enclosure the smoke can travel large vertical distances, affecting multiple floors simultaneously and threatening the life safety of occupants far way from the fire origin. Also, atrium layout intrinsically does not allow for vertical compartmentation and, thus, fire could spread to interconnected floors. Moreover, detection, control and extinguishment of fires in atria differ significantly from those in small enclosures. These complex and non conventional architectonical elements, like many others in modern buildings, can lead to fire environments that diverge significantly from those assumed in current codes and standards and most engineering calculation methods. With such remarkable

architectural features, the fire dynamics in one building does not necessarily correspond to the fire dynamics in another building. Thus, a proper understanding of fire dynamics and smoke movement for each particular building is needed to provide the scientific understanding required in the proper design of fire-safe structures [2].

Smoke inhalation is the main cause of fatalities in indoor fires. The protection of occupants from smoke can be enhanced by smoke exhaust systems, which objective is to maintain evacuate smoke and provide safer evacuation routes [3]. In most of the buildings with large interior spaces, smoke is exhausted via the top of the atrium by means of natural ventilation and/or mechanical exhaust systems (i.e. fans) [4]. Mechanical exhaust systems are used in many fire protection strategies because their performance does not depend significantly on atmospheric conditions. However, these systems are expensive and complex to design and operate, requiring analysis of smoke dynamics before a decision on their installation is taken.

The study of smoke movement in atria is most complete by conducting physical experiments. However, testing in full-scale enclosures is too complex, expensive and labour intensive, resulting in a very small number of tests that can be reasonably carried out. Reduced-scale testing [5] is a useful method to study flow in large facilities but in case of fire it is not easy to fully preserve the fluid, thermal and radiant similarities at the same time [6]. Simple analytical and empirical correlations exist for smoke movement in atria [7, 8] but these only provide general behaviour and are usually not valid for complex designs like those in modern buildings. The last option, computer modelling, consists on investigating smoke movement via computational fluid dynamics (CFD) or zone modelling simulations of smoke movement in the particular building under design [9]. Fire simulations require validation studies against real-scale tests to asses its range of applicability and accuracy.

The current international trend in fire protection engineering regulations is towards performance-based design and risk-informed analysis [10]. Performance-based design is especially significant for prestigious and iconic building types, for which building industry is constantly seeking more robust and more reliable methodologies to establish stronger links between the design and the actual performance of the building. This assessment of performance is gaining greater importance to insurers, clients, regulators and the general public. Because the shift towards performance-based codes and the difficulty of testing in atria, fire models are increasingly being used for developing fire safety engineering solutions. These models are engineering tools that can be used to investigate unconventional and innovative features in new design or non-trivial changes to existing designs.

Current development of performance-based and risk-informed fire protection needs more validation studies of fire modelling in atria. For this end, it is essential to generate more reliable and comprehensive full-scale tests for the ongoing validation of fire models [9].

Several full-scale experiments of fires in atria and large enclosures have been reported recently [11-17]. Chow et al. conducted a large set of tests at the PolyU/USTC Atrium [11], which is 27 m high. These experiments include the study of the natural smoke filling process [12], the effectiveness of mechanical smoke exhaust systems [13], as well as the influence of make up air [14]. Shi et al. [15] investigated the spill plume and natural filling of an atrium for fires in small shops ranging from 0.4 to 0.6 MW. Hostika et al. [16] conducted tests at the 19 m high VTT atrium varying systematically the fire location and the fire size between 1 and 5 MW. Lougheed and McCartey [17] conducted a series of full-scale experiments at the NRC Burn Hall facility

(12.2 m high) to investigate the smoke flow in balcony spill plumes and the resulting mechanical exhaust requirements for fire in the range from 0.5 to 5 MW.

The main aim of this work is to report new experimental results and modelling to fill the gap in experimental data and scientific understanding. The three fire tests conducted as part of the Murcia Atrium Fire Tests are presented. The facility is the 20 m cube atrium of the Centro Tecnológico del Metal, Spain. In the first two tests, the mechanical smoke exhaust system was operated. In the third test, smoke was evacuated only via natural ventilation through the openings. Detailed transient measurements of gas and wall temperatures at different heights, as well as the pressure drop through the exhaust fans and airflow at the inlets are reported here. Additionally, CFD simulations of the experiments are presented using FDS4.

2.- Murcia Test Facility

The Murcia Atrium Fire Tests have been carried out in the atrium [18] of the Centro Tecnológico del Metal, in Murcia, Spain (Figure 1) with pool fires of two sizes. This full-scale facility consists of a prismatic structure of 19.5 m x 19.5 m x 17.5 m and a pyramidal roof raised 2.5 m at the centre. The walls and roof are made of 6 mm thick steel and the floor is made of concrete. There are four exhaust fans installed on the roof, each with a diameter of 0.56 m and a nominal flow rate of 3.8 m^3/s. There are eight grilled vents arranged at the lower parts of the walls. Each vent has dimensions of 4.88 m x 2.5 m. A drawing of the rig with dimensions is shown in Figure 2.

Figure 1. Photo of the 20 m high atrium facility used in the Murcia Atrium Fire Tests, Murcia, Spain.

In order to study the fire-induced thermal and flow fields, sixty one sensors were installed measuring gas phase, walls and roof temperatures, as well as the pressure drop at exhaust fans and flow velocities at the vents. Measurements of plume temperature were taken with 3 mm-diameter bare and sheathed type K thermocouples. Both bare and sheathed thermocouples were used at each location for comparison and to assure reliability of the measurements. For

temperature measurements near the walls, vents and exhaust fans, 6 mm diameter class B bare Pt100 thermistor probes were used. Measurements of surface temperature were taken with 6 mm diameter type K thermocouples. Differential pressure transmitters were installed at the exhaust fans to measure gas flow. Hot wire anemometers were used to measure air velocity at the vents. A Modicom TSX Premium automaton connected to a PC was used to register the data with a frequency of 5 Hz. Two cameras were also installed to record the flame shape and height.

Weather conditions were measured by means of a meteorological station monitoring the wind velocity, temperature, humidity and pressure outside the facility.

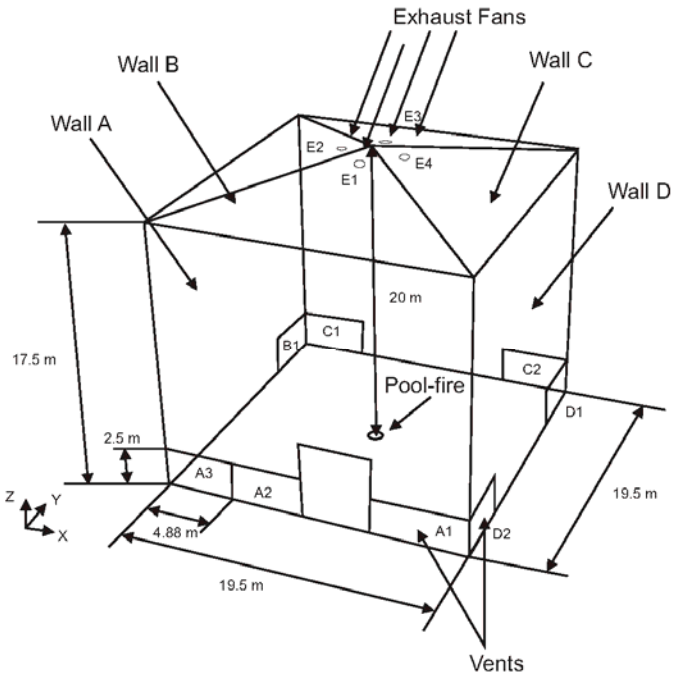

Figure 2. Layout and main dimensions of the Murcia Test facility.

The layout of the sensors used was the following (see Figure 2 for locations):

- Wall A contained nineteen sensors (Figure 3). Four thermocouples for wall temperature, nine Pt100 for air temperature 30 cm from the wall, and one Pt100 and one anemometer at each of the vents.

doi:10.1016/j.buildenv.2008.12.010

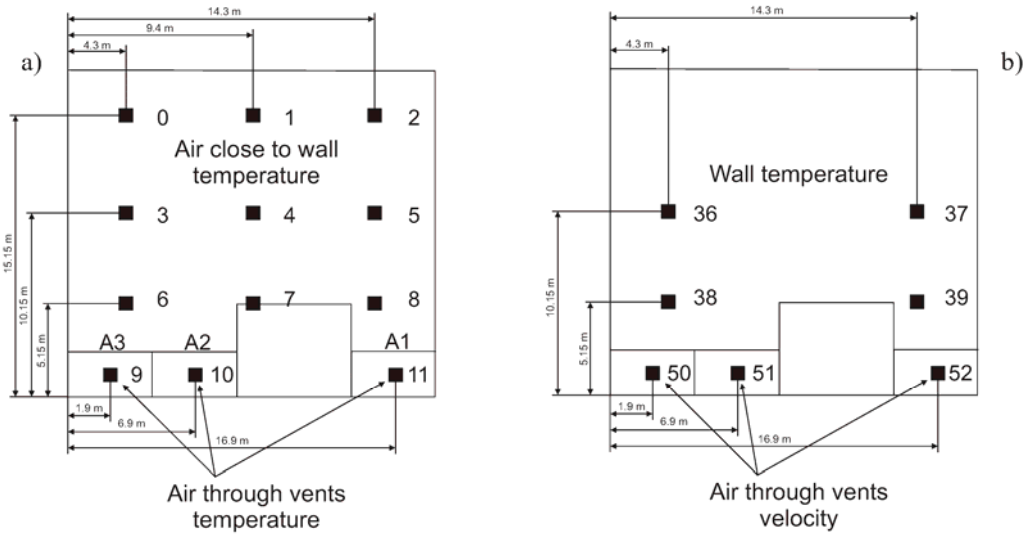

Figure 3. Sensors layout on wall A: air temperature close to wall in a), and wall temperature in b). View from the outside.

- Wall C contained eighteen sensors (see Figure 4). Four thermocouples for wall-temperature, ten Pt100 for air temperature 30 cm from the wall, and one Pt100 and one anemometer at each of the vents.

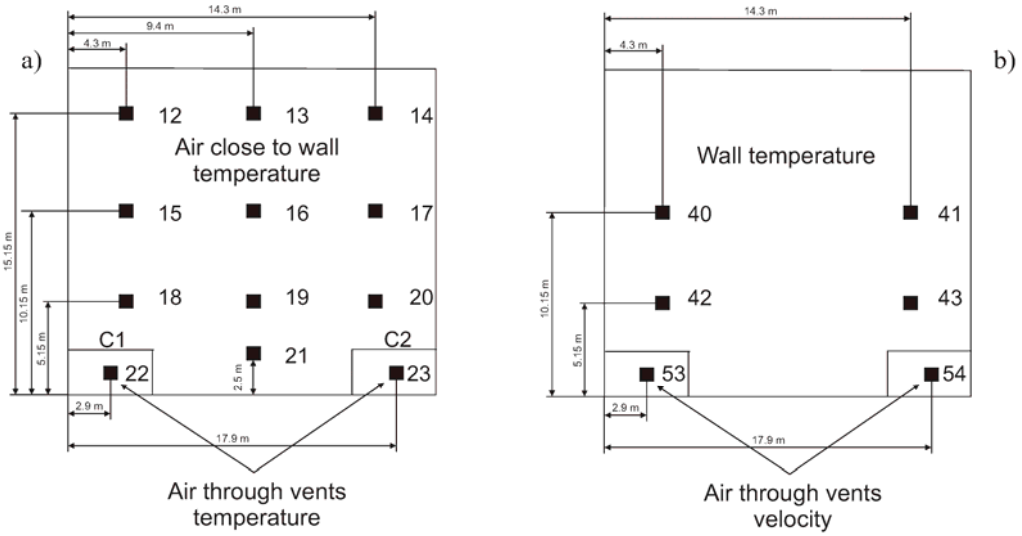

Figure 4. Sensors layout on wall C: air temperature close to wall in a), and wall temperature in b). View from the outside.

- The central section contained nine thermocouples located at three different heights (Figure 5 a). In each horizontal line there were three thermocouples. At the plume region bare and sheathed

thermocouples were installed at the same location. Near the plume region bare thermocouples were installed.

- The roof and exhaust fans contained twelve sensors (Figure 5 b). Six thermocouples measured roof temperature. Two different pressure sensors were installed at the exhaust fan close to wall A (E1) and the one close to wall C (E3). Absolute and differential pressure through them were measured in order to calculate the exhaust flow rate. One Pt100 thermistor was also installed at E1 and E3 to measure the exhaust flow temperature.

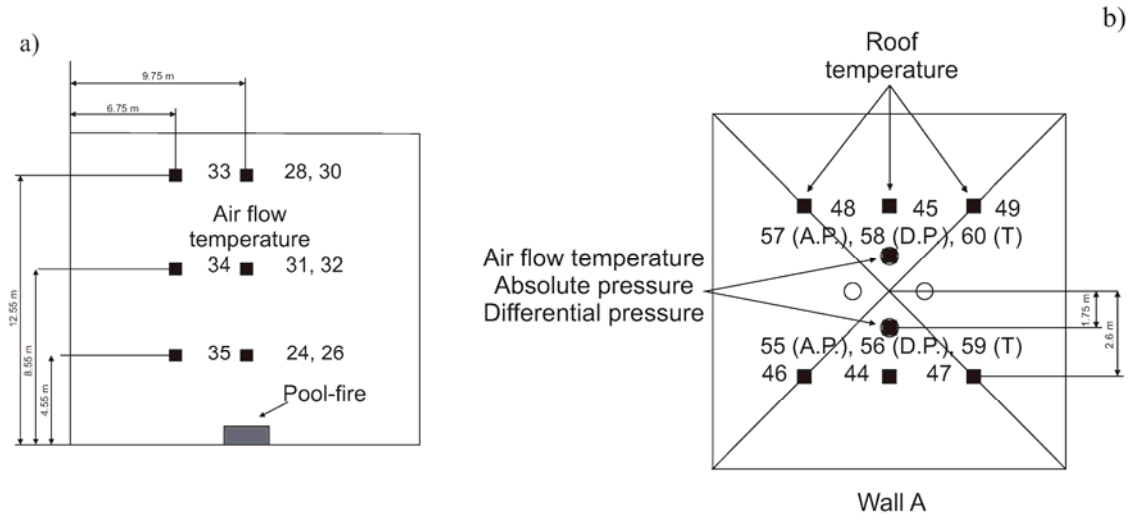

Figure 5. Layout of the central section as seen from wall A in a), and roof sensors' layout as seen from the top in b). Absolute pressure (AP), differential pressure (DP) and temperature (T).

A video camera and a webcam were placed near the walls looking towards the flame, that is, the centre of the atrium floor.

An uncertainty analysis for the measurements was conducted (see [18] for details). The analysis shows that the total experimental uncertainty for the thermocouples is 1.5%, for the thermistors is 0.4%, for the velocity probes is 4%, for the mass flow in fans is 10% and for the mass loss is 1%. The radiation correction on temperature measurements can be neglected as shown in [19] since the average errors are small, lower than 5% for temperature below 800 °C and lower than 7 % for the worst cases of very high temperatures (above 1300 °C).

3.- Description of the Fire Tests

Results from three atrium fire tests conducted on the 4th and 7th of April 2008 are presented. The burning fuel was heptane contained in circular steel pans placed at the centre of the atrium floor. The pans were 0.25 cm deep. Two different diameters pool-fires were used, 0.92 m in the first test and 1.17 m in the last two tests. In all tests, a layer of 2 cm of water was added to the pan before the heptane was poured to insulate the metal from the burning pool heat, thus providing a more stable steady burning regime. At the end of each test, the volume of water was measured again to confirm that no water had been lost. A summary of the laboratory and ambient conditions during the tests is presented in Table 1.

Fire test	Pool diameter (m)	Volume of heptane (l)	Burning time (s)	Venting conditions		Ambient conditions			Weather	Wind speed (m/s)	Calculated average HRR (MW)
				Open vents	Exhaust fans on	Temperature. (°C)	Pressure (mbar)	Hummidity (HR) (%)			
Test 1	0.92	52	1010	A1, A3, C1, C2 100%	E2, E4	13.0	1014	43	Cloudy	0.00	1.32
Test 2	1.17	75	843	A1, A3, C1, C2 100%	E2, E4	18.0	1014	47	Cloudy	0.85 – 1.00	2.28
Test 3	1.17	100	1094	A1, A3, C1, C2 100%	None, natural ventilation	16.0	997	49	Cloudy	0.00 – 0.75	2.34

Table 1. Summary of laboratory and ambient conditions during the Fire Tests.

The heat release rate (HRR), $\dot{Q}$, is the most important variable to characterize a fire. For these experiments, it is calculated by:

$$\dot{Q}(t) = \dot{m}(t)\chi_{eff}\Delta H_c . \quad (1)$$

where $\dot{m}$ is the mass loss rate of the fuel, ΔH_c is the heat of combustion and χ_{eff} the combustion efficiency. The heat of reaction of heptane for complete combustion is 44.6 MJ/kg [7]. The combustion efficiency expresses the difference between theoretical heat of combustion and the effective heat of combustion. It generally depends on the fuel, the soot production, the ventilation conditions and the flame size [7]. Experimental results in [20] show that χ_{eff} for well-ventilated pool fires is weakly dependent on pool fire diameter within the range of 0.1 – 2 m. Hostikka *et al.* [16] reported a value of 0.8±0.1 for well-ventilated heptane fires ranging from 0.71 m to 1.60 m in diameter. In [21], a combustion efficiency of 0.85±0.12 is suggested for heptane fires of 1.2 to 1.6 m in diameter. Based on these results, for the present work, a combustion efficiency of 0.85 is chosen.

The instantaneous mass loss rate, $\dot{m}(t)$, was not measured directly due to the weight limitation of the available balance. Instead, the average mass loss rate, $\overline{\dot{m}}$, for each test was measured as the total mass of fuel burnt divided by the burning time. The evolution of the instantaneous mass loss rate was recovered from the measurements of mass loss in a smaller pool fire, 0.55 m diameter. This evolution is then normalized as:

$$\dot{\omega}(t) = \frac{\dot{m}(t)}{\overline{\dot{m}}} \quad (2)$$

where $\dot{\omega}(t)$ is the normalized instantaneous mass loss rate. Figure 6 shows the evolution of the normalized mass loss rate for the 0.55 m pan and for measurements for a wide range of pool fire by Hostika *et al.* [16]. This comparison shows that the normalized mass loss rates for pool fires in

the range from 0.55 to 1.17 m diameter collapse in one curve. Each pool size shows a different burning time proportional to the initial volume of fuel in the pan. The normalized evolution was used to calculate the mass loss rate in each of the three fire tests and the heat release rate calculated using Eq. (1) and shown in Figure 7. The resulting steady-state heat release rates were 1.32 MW, 2.28 MW and 2.34 MW, respectively. The uncertainty associated with the heat released rate is estimated to be around ± 15 %.

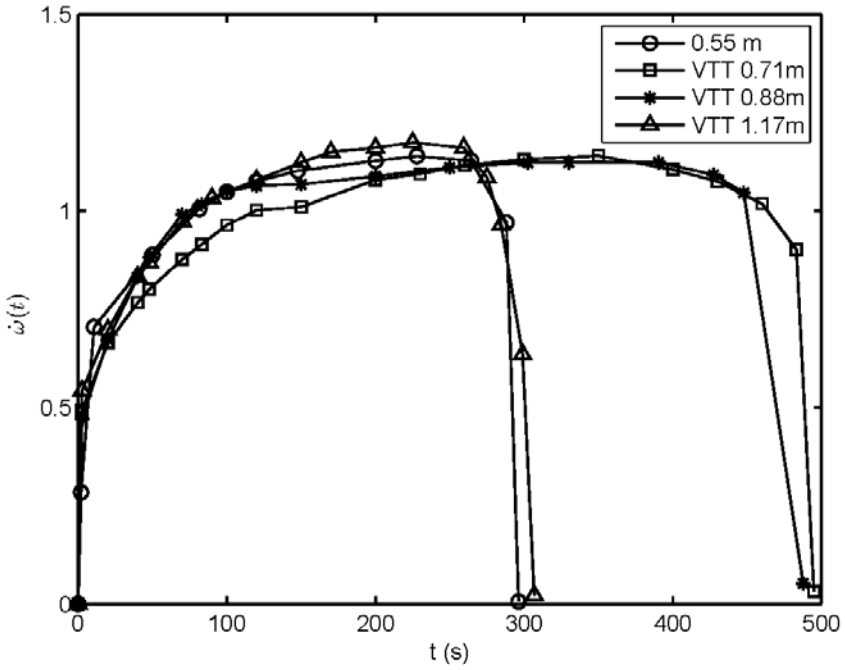

Figure 6. Comparison of normalized mass loss rates, $\dot{\omega}(t)$, as measured for different heptane pool diameters. VTT results in [16].

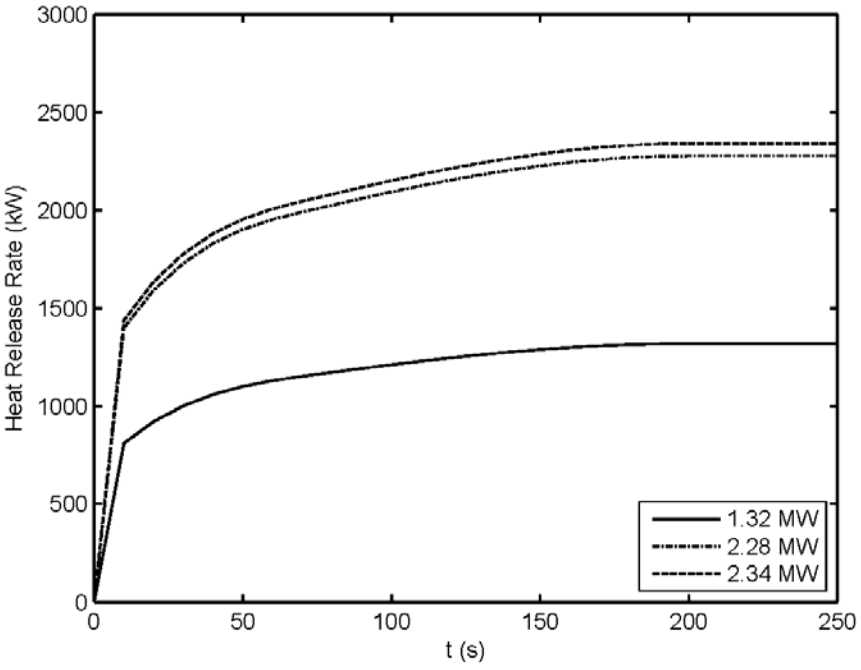

Figure 7. Detail of the initial stage of the heat release rates estimated using Eq.(1) and the normalized mass loss rate from Eq. (2) shown in Figure 6.

The flame height was also measured and compared with the empirical correlation for pool fire from [7] seen in Eq. (3):

$$\frac{L}{D} = -1.02 + 3.7 \cdot \dot{Q}^{*2/5} \quad , \tag{3}$$

where L is the flame height, D is the pool diameter, and Q^* is the Froude number of a fire defined as,

$$\dot{Q}^* = \frac{\dot{Q}}{\rho_\infty c_p T_\infty \sqrt{gD} D^2} \quad , \tag{4}$$

where ρ_∞ and T_∞ are the ambient density and temperature, respectively, c_p is the specific heat of air and g is the gravity acceleration.

For Test 1, the flame height in the steady burning period was measured in the range 2.8 - 3.5 m (Figure 8 a). This value agrees well with the prediction of 3.3 m for a 1.32 MW fire in a 0.92 m pan provided by Eq (3). The flame height of Test 2 ranged during the steady burning period from 3.8 m to 4.6 m (Figure 8 b). This value agrees well with the prediction of 4.1 m from Eq. (3). The flame height of Test 3 (Figure 8 c) was similar to that in Test 2, ranging from 3.8 m to 4.6 m and agrees well with the prediction of 4.2 m.

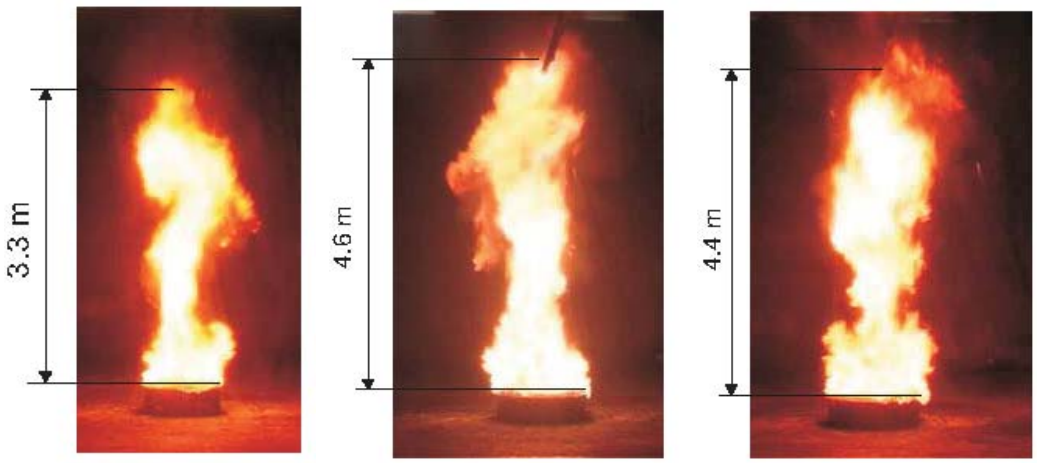

Figure 8. Snapshot showing the flame heights during the steady-state of the tests. Test 1, 0.92 m pool and 1.32 MW fire in a), Test 2, 1.17 m pool and 2.28 MW fire in b), and Test 3, 1.17 m pool and 2.34 MW fire in c).

The complete set of measurements from the experiments is shown and discussed in section 5 of the paper, after the description of the fire simulations.

4.- Description of Fire Simulations

4.1.- Mathematical Model

Simulations of the three fire tests have been performed to compare with the experimental results. The CFD code used is FDS4 developed at NIST [22]. The code is widely used in fire protection engineering. The turbulence is modelled using a large-eddy simulation (LES) approach [23], and the combustion model is based on the mixture fraction approach that assumes the combustion is mixing-controlled. The radiative heat transfer is computed by solving the radiation transport equation for a non-scattering grey gas.

The computational domain includes the atrium space, the walls and the roof. The heat release rate is prescribed in the input as a function of time following the results in Figure 7. The radiative fraction is set to 0.35 which is the value experimentally measured for similar heptane fires [12, 24]. The grilled vents and inactive exhaust fans have been simulated as openings to the atmosphere at ambient pressure. The active exhaust fans were simulated as vents with a constant velocity across their area providing the nominal flow rate of 3.8 m^3/s specified by the manufacturer. The walls and roof were modelled as steel sheets (density of 7800 kg/m^3, thermal conductivity of 45 W/K m, specific heat of 460 J/kg K and emissivity of 0.3 [25]) with a thickness of 6 mm. The floor is modelled as a thick layer of concrete (density of 1860 kg/m^3, thermal conductivity of 0.72 W/K m, specific heat of 780 J/kg K [25]). Other parameters in FDS4 have been left as the default values.

4.2.- Grid Sensitivity Study

The grid used is one of the most important numerical parameter in CFD [22] dictating its numerical accuracy. The necessary spatial resolution for a proper LES simulation is customary defined in terms of the characteristic diameter of a plume [21], which is defined as [7],

$$z^* = \left(\frac{\dot{Q}}{\rho_\infty c_{p,\infty} T_\infty \sqrt{g}} \right)^{2/5}. \tag{5}$$

The special resolution R^* of a numerical grid is defined as,

$$R^* = \frac{\Delta x}{z}. \tag{6}$$

where Δx is the characteristic length of a cell for a given grid. The necessary resolution suggested in most studies is between 1/5 and 1/10 [21, 22]. Other studies [26] suggested resolution of 1/20 to successfully predict the flame height. For this work, a resolution between 1/10 and 1/15 has been chosen, which results in the number of grid cells shown in Table 2.

Fire test (MW)	Cells number for $R^* = 1/5$	Cells number for $R^* = 1/10$	Cells number for $R^* = 1/15$
1.32	83	167	250
2.28	67	135	202
2.34	67	133	200

Table 2. Number of cells needed in each direction for different grid resolutions.

In the grid sensitivity studies conducted here, the size of the cells in the grid has been systematically reduced until a compromise solution between numerical accuracy and computational time is achieved. Six grids have been studied, 40 cells, 60, 90, 120, 150 and 180 cells per side of the cubic atrium (*i.e.* 20 m). For the sake of simplicity, the grid sensitivity study has been conducted with steady-state fires at two heat release rates (1.3 and 2.3 MW). The heat release rate is set constant and 100 s are simulated for each grid size. Then, the temperatures have been averaged for the last 80 s at each height of interest. Results have been compared between them to quantify grid independence. In LES is not possible to archive perfect grid independence although little variations can be theoretically expected between grids if they are fine enough [23, 27]. Tables 3 and 4 show the temperature predictions in the atrium for each grid. The plume temperature at 5 m high varies considerably with the grid size. This location is sometimes reached by the flame and is not expected to be accurate due to the difficulties of modelling accurately the near field of a flame using FDS4 [22]. For both fire powers, the temperatures at 13 m high and at the exhaust fans vary significantly for the three coarser grids, while it is fairly independent for grids finer than 120 cells per side of the atrium. This is equivalent to cubic cells smaller than 0.17 m in length. It is concluded then that finer grids than this one are not required in order to capture the far field temperature high in the atrium but will only increase the computing time required.

Height	**Temperature predictions (ºC)**						**Relative error respect to finest grid (%)**				
	40 cells	**60 cells**	**90 cells**	**120 cells**	**150 cells**	**180 cells**	**40 cells**	**60 cells**	**90 cells**	**120 cells**	**150 cells**
Exhaust fan	49	66	64	53	58	56	13	18	14	5	4
Plume at 13m	64	110	99	78	81	74	14	49	34	5	9
Plume at 9m	80	152	173	129	160	136	41	12	27	5	18
Plume at 5m	116	226	333	293	503	487	76	54	32	40	3

Table 3. Centreline plume temperatures at different heights as a function of the grid size for a 1.3 MW fire. Grids are expressed as number of cells per atrium side (20 m)

Height	**Temperature predictions (ºC)**						**Relative error respect to finest grid (%)**				
	40 cells	**60 cells**	**90 cells**	**120 cells**	**150 cells**	**180 cells**	**40 cells**	**60 cells**	**90 cells**	**120 cells**	**150 cells**
Exhaust fan	58	72	67	60	59	56	4	29	20	7	5
Plume at 13m	110	126	111	114	88	75	47	68	48	52	17
Plume at 9m	143	193	221	262	200	142	1	36	56	85	41
Plume at 5m	174	259	448	582	646	540	68	52	17	8	20

Table 4. Centreline plume temperatures at different heights as a function of the grid size for a 2.3 MW fire. Grids are expressed as number of cells per atrium side (20 m)

Comparison of the results for different grids shows that the relative error between grids is big for the three coarser ones. For the 1.3 MW fire, the relative errors between the finer grids of 150 cells per side and 180 cells per side are lower than 10 % at 13 m high, and lower than 5 % at the exhaust fans. For the 2.3 MW fire, the discrepancy between the finer grids is lower than 20 % and 5 %, respectively. Thus, it is concluded that any of the two finer grids is valid for simulating the fire. Taking into account the criterion of special resolution between 1/10 and 1/15, the 180 cells per side was chosen for the 1.3 MW fire and the 150 cells per side for the 2.3 MW fire.

Additionally, and to verify that the grids are fine enough to provide accurate results, the results have been compared with the values from plume theory provided in [28]. Table 5 shows the relative errors for each grid and fire sizes. It is seen that the predictions agree better with the plume correlation for finer grids and at higher locations. Close to the flame, the agreement is poor. Figure 9 plots the results contained in Tables 3 and 4, and predictions from plume theory. It shows that the coarser grids do not predict well the plume temperature. It is not until the grid of 90 cells per side that some agreement can be appreciated. The two finest grids show the largest agreement with plume theory. The grids of 150 cells and 180 cells per side over-predict plume temperature near the flame (5 m high). They also over-predict plume temperature below 9 m high. The overprediction is reduced at the upper parts of the atrium, which are the most important for smoke evacuation in atria, showing good agreement. It is concluded then that the selected grids of 150 and 180 cells per side provide good accuracy with an error smaller than 10% above 13 m from the ground as compared to the plume correlations.

	Relative error respect to plume correlation (%)											
Height	**1.3 MW**						**2.3 MW**					
(m)	**40 cells**	**60 cells**	**90 cells**	**120 cells**	**150 cells**	**180 cells**	**40 cells**	**60 cells**	**90 cells**	**120 cells**	**150 cells**	**180 cells**
5	59.5	21.0	16.7	2.7	76.4	70.5	57.0	36.1	10.4	43.4	59.2	33.1
9	30.0	33.6	51.6	12.8	42.3	18.5	0.3	35.2	54.8	83.2	41.5	1.3
13	11.9	51.0	35.5	6.5	12.2	0.4	34.4	53.1	36.1	40.0	10.1	9.7
17	13.1	16.2	13.9	6.2	2.5	1.1	1.1	24.7	15.5	2.4	2.5	4.9

Table 5. Relative errors in the centreline plume temperature respect to plume correlation [28]. Grids are expressed as number of cells per atrium side (20 m)

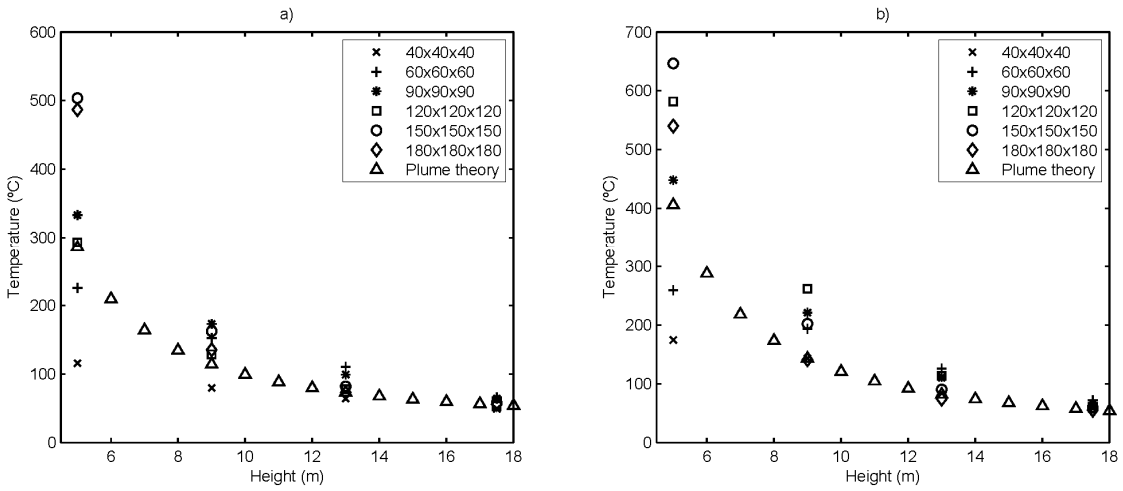

Figure 9. Comparison of predicted plume temperatures for different grid sizes for the the 1.3 MW fire in a), and for the 2.3 MW fire in b).

A final proof of the goodness of the grids used is provided in the next section of the paper which includes a comparison between experiments and FDS predictions for different grids at different locations, for the 1.3 MW fire (see Figure 10). The agreement between experiments and the grids of 150 cells and 180 cells per side is good, confirming the results from the grid sensitivity and spatial resolution requirements.

The influence of the number of solid angles used for radiative heat transfer computation has been also studied. As default, FDS divides the grid into 100 solid angles. Other numbers of solid angles, 200 and 300, have been tested but the improvement has been marginal. Thus, the default division of 100 solid angles has been used.

5.- Experimental and Computational Results

At present section, experimental results from the three Fire Tests as well as comparison with predicted results from FDS are presented and discussed. Results in three key regions are reported: the plume temperature, the exhaust smoke temperature, and the smoke layer temperature by means of the temperature of the air close to the walls. The smoke layer height in the experiments is calculated using the N-percent method [29]. Temperature-time evolutions at different locations are presented for Test 1, in Table 6, Test 2, in Table 7, and Test 3, in Table 8.

Figure 10 compares the temperature measurement in the plume of the 1.3 MW with the FDS predictions using different grids and shows the robustness of the grid analysis and provides confidence that the grid size is correct. Figures 11, 13 and 15 report the temperatures of the plume for both 3 mm bared (sensors 24, 28, 31) and sheathed (sensors 26, 30 and 32) thermocouples measurements. In general, the agreement between both thermocouple types is good (lower than 10 %). This fact reflects on the accuracy of the measurements and their reliability.

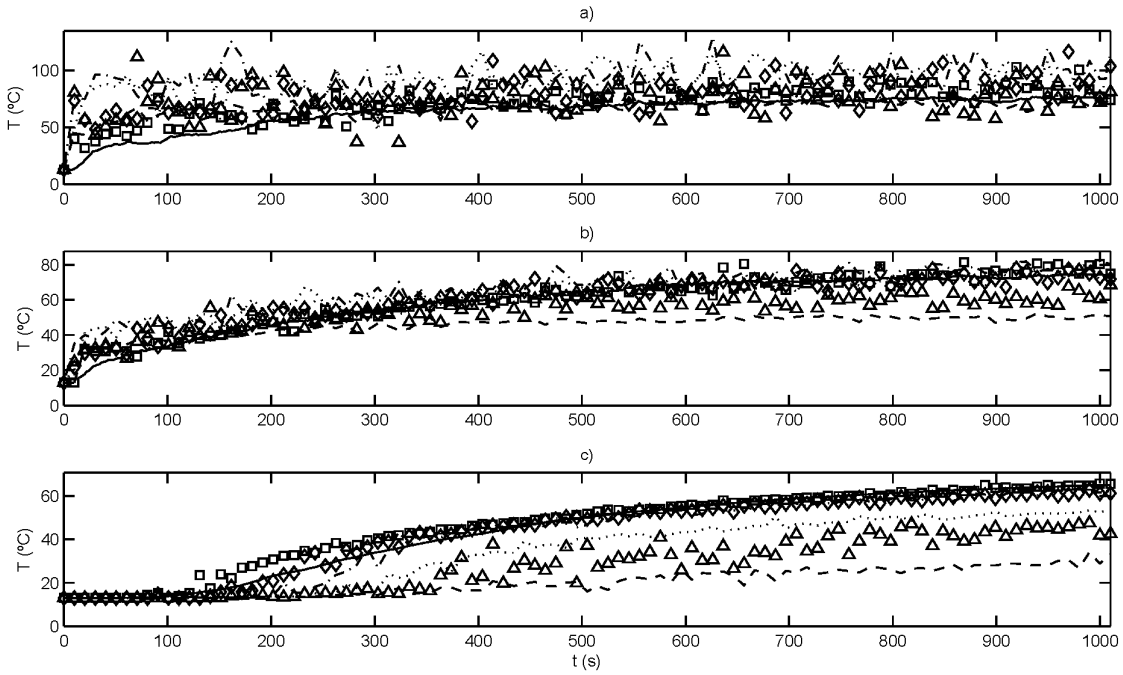

Figure 10. Comparison of temperature measurements and predictions for different grid sizes for the 1.3 MW fire at the plume 12.55 m high in a), fans in b), and 10 m high near wall A in c).

doi:10.1016/j.buildenv.2008.12.010

Experiments in solid line; grid of 40 cells per side in dashed line; 60 cells per side in dotted line; 90 cells per side in dash-dot line; 120 cells per side in triangle; 150 cells per side in diamond; 180 cells per side in square.

Next, each of the fire tests is discussed separately.

- **Test 1:**

Test 1 is with the pan of 0.92 m. Two fans on the roof were activated (E2 and E4) and the other two were inactive (E1 and E3) but their opening acted as vents for natural ventilation. Figures 11 and 12 show the measurements and predictions vs time.

Time	Sensor number									
(s)	24	31	28	60	1	4	7	13	16	19
0	10.4	10.8	12.6	14.8	13.5	12.9	12.6	13.6	13.2	12.8
67.4	110.1	50.9	36	30.5	17.6	13.1	13	17.8	13.5	13.1
134.9	153.2	61	43.6	39.4	26.3	15.9	13.8	26.2	16.4	13.9
202.3	224	80.2	55.4	46	33.9	23.2	15.1	33.6	23.7	15.3
269.8	218.7	78.6	61.2	51.5	40.4	30.7	16.7	40.7	31.4	16.8
337.2	223.6	76.5	63.4	56.1	45.9	37.4	18.7	46.9	36.7	18.6
404.7	196.4	77.4	66.1	59.8	51.2	42.8	20.8	51	42.4	20.6
472.1	198	77.4	66.3	63.4	55.1	48.4	22.6	54.4	48.2	22.1
539.6	186.2	78.6	70	65.5	57.8	52.2	24.3	57.1	52.4	23.6
607	187.8	80.6	70.8	68.9	59.8	55.2	25.5	60.5	55.8	24.1
674.5	192.3	81.1	72.7	69.9	62	57.8	26.4	62.8	57.9	24.9
741.9	181.7	81.3	73.1	70.7	63.6	59.8	26.2	64.3	60.6	25.3
809.3	225.2	84.3	74.9	72	65.2	61.4	26.6	65.3	62.1	25.8
876.8	196.9	78.7	74.2	73.5	66.5	62.8	27	66.4	63.4	26.2
944.2	199.6	82.3	75.7	73.8	67.5	64.1	27.4	67.1	64.6	26.4

Table 6. Time-temperature measurements for different sensors in Test 1 – 1.3 MW, values in °C. See Figures 3-5 for sensor labels.

Figure 11 compares results for the plume temperature at central line of the atrium and at the exhaust fans. It shows that plume temperatures at the lower heights (below 9 m) are relatively constant after a short transient (after 200 s). The temperature at the exhaust fans (Figure 11 d) shows that the smoke reaches the ceiling about 10 s after ignition. The smoke temperature increases slowly to 75 °C and after 850 s, it reaches quasi steady-state.

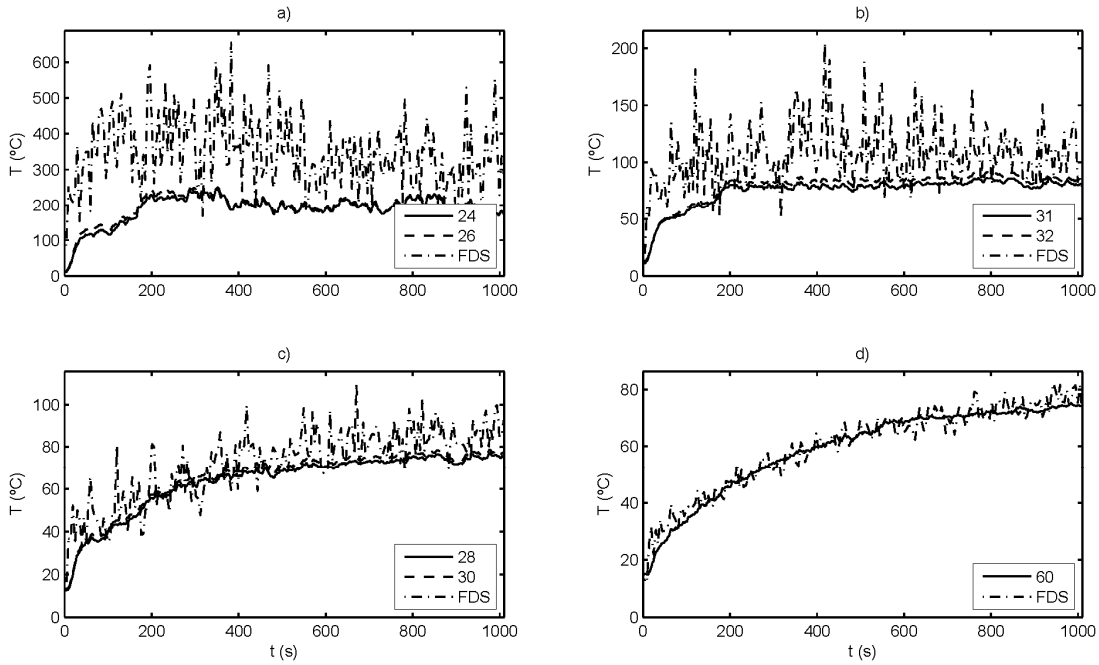

Figure 11. Temperature measurements and predictions at the plume and exhaust fans for Test 1 – 1.3 MW. 4.55 m high in a); 8.55 m high in b); 12.55 m high in c); Exhaust fan in d). Measurements are for both bare and sheathed thermocouples and identified by sensor number according to Figure 5.

Figure 12 shows temperature results near the wall for two different walls. They show the built up of the hot layer. This is due to the smoke exhaust rate at the top being lower than the flow along the plume at the roof height. The temperature rises first at 15 m high at 25 s, as the ceiling jet reaches first this location. Then, the smoke layer continues growing, and temperature starts to rise at the height of 10 m at 60 s and, finally, at the one of 5 m at 80 s.. Comparison of the measurements at symmetrical wall position shows a strong spatial symmetry since the evolution is almost identical. This observation implies that the plume and the smoke layers were not affected by flow perturbations during the test. Applying the N-percent method [29] to the temperature measurements near the walls, the smoke layer height can he calculated (Figure 12 d). It has been assumed different values for N, 10 % and 20 % as in [29] and 30 % as in [14]. It is observed that after 200 s the smoke layer reaches the height of 5 m for the most conservative assumption.

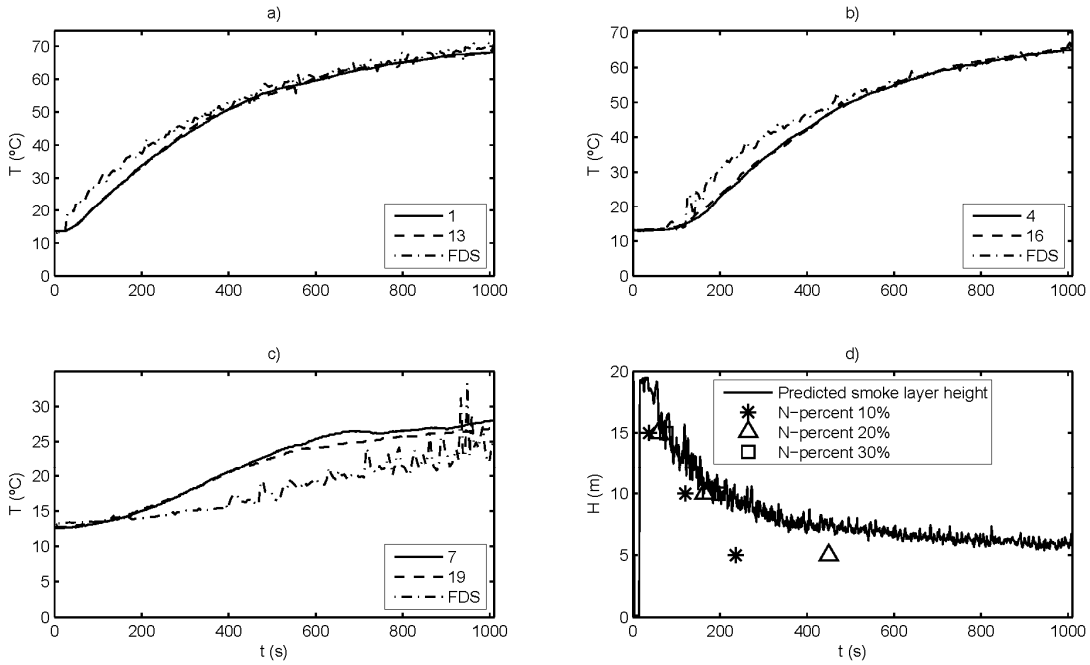

Figure 12. Temperature near the walls and smoke layer height measurements and predictions for Test 1 – 1.3 MW. Temperatures 15 m high in a); 10 m high in b); 5 m high in c); and smoke layer height in d). Measurements are for symmetrical locations at walls A and C and identified by sensor number according to Figures 3 and 4.

The numerical simulation over-predicts the plume temperature near the flame and the lower plume heights by more than 20 %. The relative error at h = 4.55 m (Figure 11 a), ranges from 40 to 50 %, at h = 8.55 m (Figure 11 b) is 20 %, within the error associated to FDS, and at h = 12.55 m (Figure 11 c) is lower than 10 %. The same conclusions are reached for the predictions of temperature at the exhaust (Figure 11 d) and near the walls (Figure 12 a-c). Predictions of smoke layer height (Figure 12 d) agree well with measurements during most of the growth period but predict a longer time to reach the height of 5 m.

- **Test 2:**

Test 2 is with the pan of 1.17 m. Two fans on the roof were activated (E2 and E4) and the other two were inactive (E1 and E3) acting as vents for natural ventilation. Figures 13 and 14 show the measurements and predictions vs time.

Time	Sensor number									
(s)	24	31	28	60	1	4	7	13	16	19
0	19	16.5	19.2	23.5	21.5	18.9	17.7	21.4	18.8	17.9
56.1	103.5	53.4	43.4	42	26.6	19.3	18.2	25.6	19.4	18.3
112.1	141.1	72	58.9	53.5	37.3	25.8	19.4	35.5	27.2	19.4
168.2	180.5	78.4	68.3	63.7	48.5	35.1	21.3	46.5	37.2	21.4
224.3	293.2	98.7	79.6	75.1	57.7	45.4	24	56.7	47.3	24.2
280.3	333.3	110	90.3	82	65.6	54.3	27.3	65.8	56.1	27.4
336.4	361.1	122.3	100.5	90.1	73.9	62.6	32	73	63.9	31
392.5	308.2	114.1	99.3	94.7	80.6	69.3	35.3	79.3	71.5	35.1
448.5	237.8	105	98.1	97.6	84.9	76	38.3	84.9	78	38.6
504.6	355	126.8	108.7	103.1	88	80	39.4	88.8	82.6	40.2
560.7	345.2	123.1	109.6	106.6	91.7	83.7	41.2	92.5	85.3	41
616.8	362.7	128.6	113.2	107.1	94.4	86.7	42.1	94.8	87.8	41.5
672.8	390.8	137.6	116.5	109.5	96.8	89.5	43	97.2	90.4	41.8
728.9	323.7	125.3	111.4	109.7	99	92	43.8	99.1	93	42.2
785	282.2	117.5	109.3	109.5	100.2	93.8	44.2	100	94.6	42.2
841	285.4	117.5	109.1	108.9	100.5	95.7	44.7	100.5	95.7	43.5

Table 7. Time-temperature measurements for different sensors in Test 2 – 2.28 MW, values in °C. See Figures 3-5 for sensor labels.

Figure 13 shows results for the plume at central line of the atrium and at the exhaust fans. The plume temperature at h = 4.55 m (Figure 13 a), and at h = 8.55 m (Figure 13 b), vary slightly during the test, indicating some small plume deviations. They are caused by ventilation asymmetries induced by the outer wind. The temperature at the exhaust fans (Figure 13 d) shows that the smoke reaches the roof about 8 s after ignition. The smoke then accumulates at the top forming a smoke layer. The smoke temperature at the exhaust fans rises to 110 °C, reaching a quasi steady-state at 650 s.

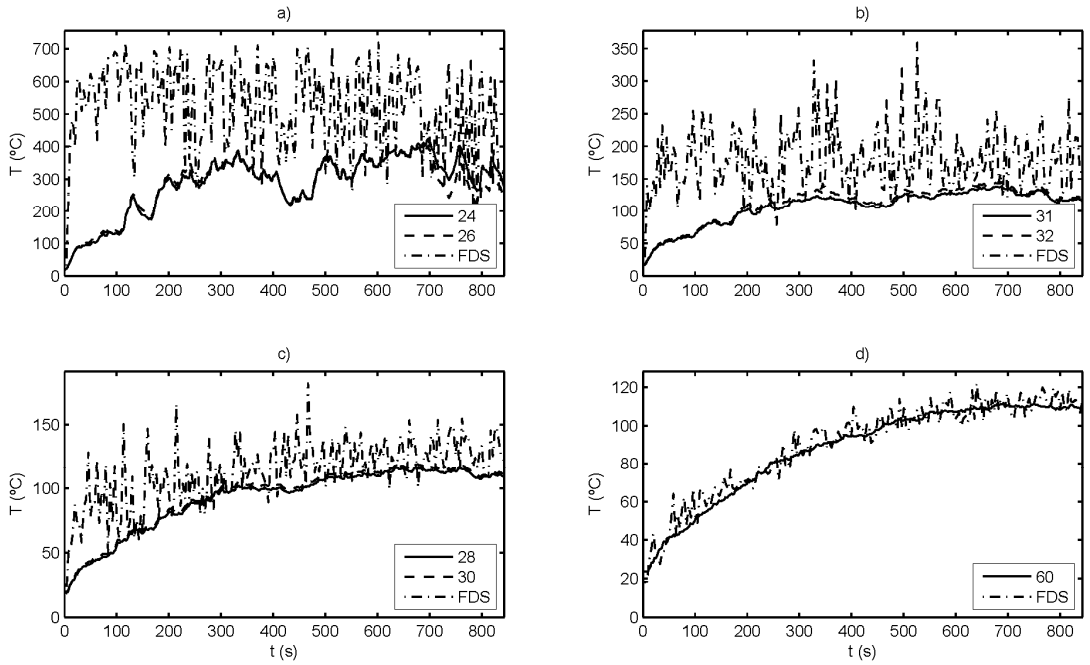

Figure 13. Temperature measurements and predictions at the plume and exhaust fans for Test 2 – 2.28 MW. 4.55 m high in a); 8.55 m high in b); 12.55 m high in c); Exhaust fan in d). Measurements are for both bare and sheathed thermocouples and identified by sensor number according to Figure 5.

The heat release rate of this test is larger than in Test 1. The smoke production is also larger and the hot smoke layer grows faster. Figure 14 shows temperature results near the walls A and C. As the smoke layer grows, the temperature starts to rise at the height of 15 m before 20 s, reaching a quasi steady-state at 700 s. The temperature starts to rise at the height of 10 m at 40 s, reaching a maximum value of 96 °C. The temperature starts to rise at the height of 5 m about 60 s after ignition. The smoke layer clearly reaches this height before 200 s for the most conservative assumption.

doi:10.1016/j.buildenv.2008.12.010

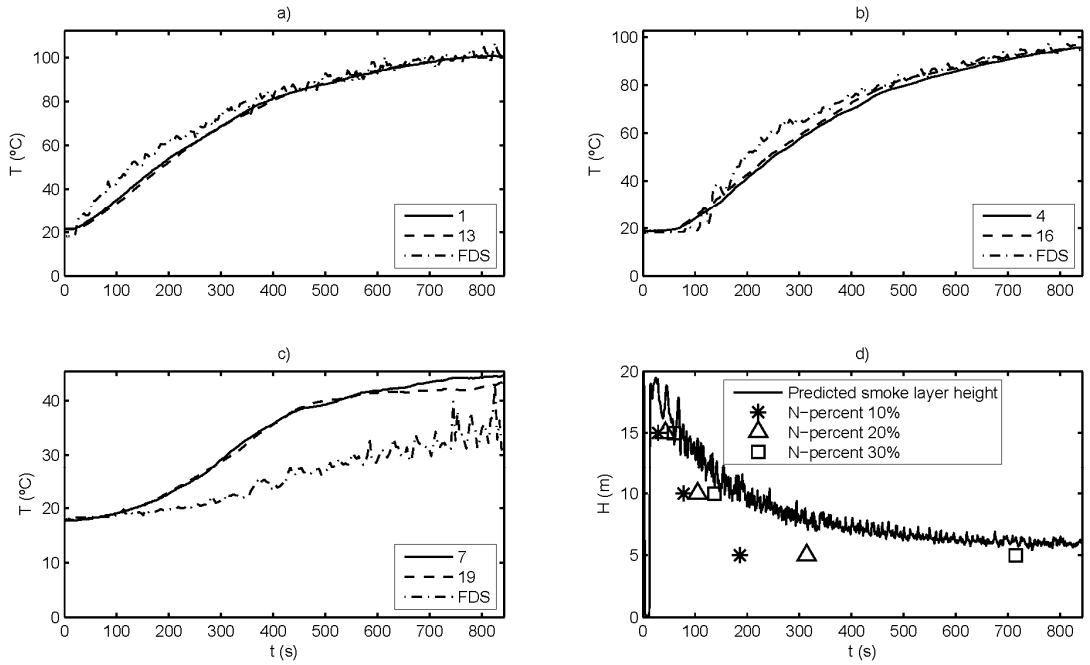

Figure 14. Temperature near the walls and smoke layer height measurements and predictions for Test 2 – 2.28 MW. Temperatures 15 m high in a); 10 m high in b); 5 m high in c); and smoke layer height in d). Measurements are for symmetrical locations at walls A and C and identified by sensor number according to Figures 3 and 4.

The plume temperatures predicted by FDS are higher than measurements. The main largest differences are found at the beginning of the fire test as happened in Test 1. Regardless of these first moments, the maximum relative errors between experiments and FDS predictions range from 50 % to 80 % at h = 4.55 m (Figure 13 a), are equal to 40 % at h= 8.55 m (Figure 13 b), and lower than 12.5 %, within FDS accuracy, at h = 12.55m (Figure 13 c). At the exhaust fans (Figure 13 d) and near the walls at the heights of 15 m (Figure 14 a) and 10 m (Figure 14 b) there is good agreement between measurements and predictions. Nonetheless, FDS slightly under-predicts air temperature at h = 5 m near the wall (Figure 14 c). The relative error is lower than 25 % respect to measurements at the end. Predictions of smoke layer height agree well with measurements for a value of N = 30 %.

- **Test 3:**

Test 3 is with the pan of 1.17 m. The four fans on the roof were inactive; thus, only natural ventilation was considered. Figures 15 and 16 show the measurements and predictions vs time.

Time	Sensor number									
(s)	24	31	28	60	1	4	7	13	16	19
0	13.3	14	15.3	16.1	16	15.9	15.9	16.1	16.3	16.1
73.3	248.8	74.1	56.3	42.9	24	16.9	16.6	24.3	17.1	16.6
146.4	294	85.4	67.3	58.3	39.3	28.1	18.3	40.2	27.9	18.4
219.5	346.6	107.8	85.9	74.6	54.4	41.6	22.1	54.9	42.7	22.2
292.7	347.3	117.5	95.2	87.4	67.9	55.5	30.1	68	54.9	30
365.8	394.1	134.4	106.9	97.6	78.9	66.8	39.5	78.2	67.6	40.4
438.9	377	133.1	109.8	103.3	87.3	75.7	49	87.1	78.1	49.7
512.1	406.3	136.6	116.9	109.9	92.8	83.1	56.6	93.8	85.7	56.9
585.2	406.7	149.3	121.8	113.7	98.1	88.8	62.4	99.5	90.5	62.4
658.3	339.1	137.4	118.6	113.8	102	93.4	67.1	103.2	95.5	66.9
731.5	407.5	151.4	127.4	118.5	104.3	96.8	68.7	104.3	98.2	68.3
804.6	425	152	130	120.9	106.9	98.9	63.6	106	100.2	62.9
877.7	423.3	150.1	127.2	119.6	108.2	101.1	60.2	107.4	102	58.8
950.9	403	141.9	125.1	119.3	109.1	102.4	59.3	108.4	103	58.5
1024	294	134.6	123.3	120.8	109.1	103.5	59	109.3	104.1	57.9

Table 8. Time-temperature measurements for different sensors in Test 3 – 2.34 MW, values in °C. See Figures 3-5 for sensor labels.

Figure 15 compares results for the plume at central line of the atrium and at the exhaust fans. This fire test shows relatively constant temperatures at the lower heights (Figures 15 a and b) at the steady combustion period. This indicates little plume deviations due to ventilation asymmetries. At the end, small plume temperature drop is observed at the lowest height (Figure 15 a) due to the effect of the wind. Temperature starts to rise at the exhaust fans (Figure 15 d) 8 s after ignition. Then, smoke starts to accumulate. The absence of mechanical ventilation causes faster smoke accumulation than in the previous test and higher smoke temperatures. After 700 s the smoke temperature reaches a quasi steady-state at 120 °C.

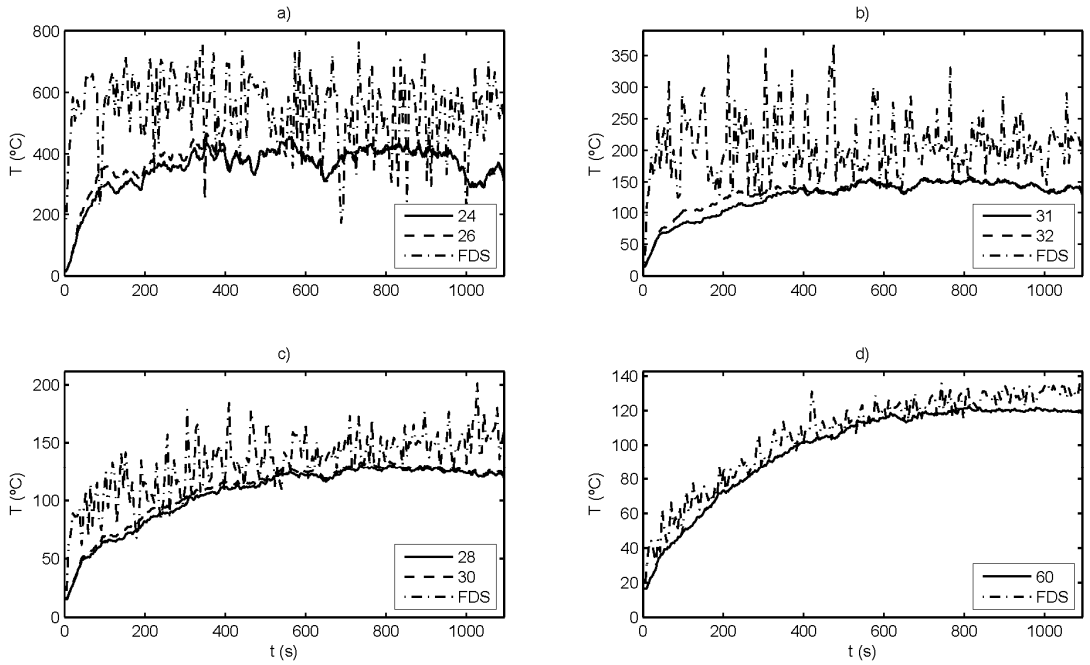

Figure 15. Temperature measurements and predictions at the plume and exhaust fans for Test 3 – 2.34 MW. 4.55 m high in a); 8.55 m high in b); 12.55 m high in c); Exhaust fan in d). Measurements are for both bare and sheathed thermocouples and identified by sensor number according to Figure 5.

Figure 16 shows temperature results near the walls. High spatial symmetry is found. Due to faster accumulation of smoke the temperature increase is larger near the walls. Temperature rises first at 15 m (Figure 16 a) high up to 110 ºC at the final moments. Smoke reaches later the height of 10 m (Figure 16 b) and temperature rises to a value of 104 ºC. The larger accumulation of smoke can be noticed at 5 m high (Figure 16 d). Temperature rises up to a maximum value of 68 ºC, at 700 s. Then, it drops to 60 ºC remaining constant until the end.

doi:10.1016/j.buildenv.2008.12.010

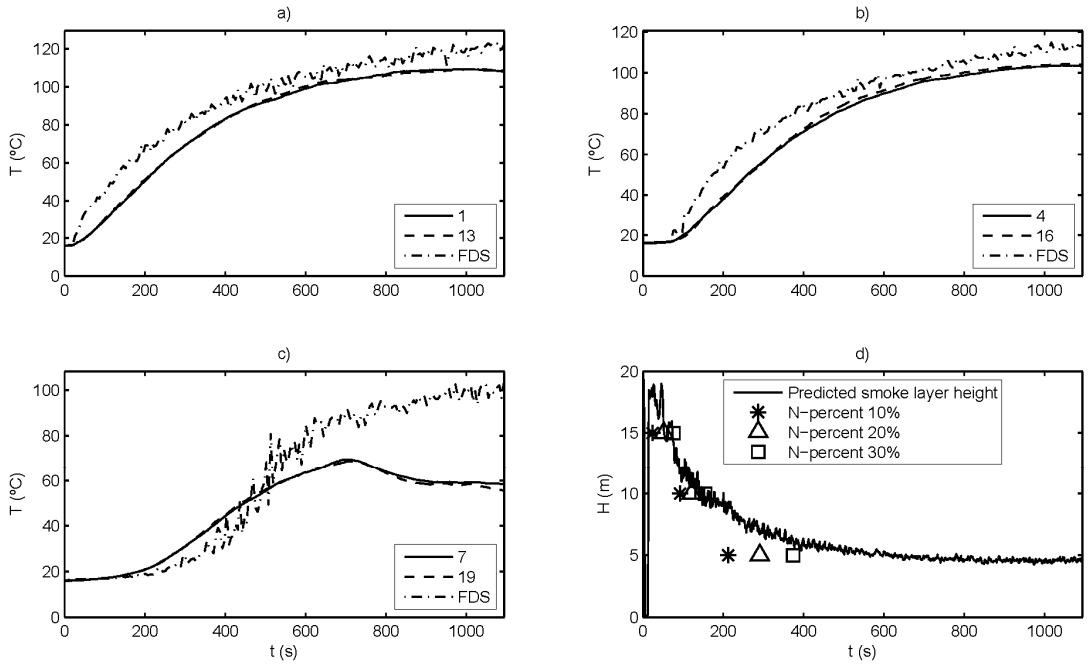

Figure 16. Temperature near the walls and smoke layer height measurements and predictions for Test 3 – 2.34 MW. Temperatures 15 m high, in a); 10 m high, in b); 5 m high, in c); and smoke layer height in d). Measurements are for symmetrical locations at walls A and C and identified by sensor number according to Figures 3 and 4.

Comparison with simulation shows that the plume temperatures predicted are higher than the measurements (Figures 15 a-c). The differences are larger at the lower parts (Figures 15 a and b). The relative error at h = 4.55 m (Figure 15 a) ranges from 50 to 80 %, at h = 8.55 m (Figure 15 b) from 35 to 45 %, and at h = 12.55 m (Figure 15 c) from 20 to 25 %. Natural ventilation is more influenced by outer effects (i.e. wind) than mechanical exhaust. Thus, larger differences between measurements and predictions than in previous test might be expected. At the exhaust fans (Figure 15 d) the predicted smoke temperature agrees well with measurements, being the relative error lower than 20 %. The numerical simulation slightly over-predicts the temperatures near the walls. For h = 15 m (Figure 16 a) and h = 10 m (Figure 16 b) still good agreement is found, with relative errors lower than 15 %, at h = 15 m, and lower than 10 %, at h = 10 m, during the steady combustion period. Higher differences are found at h = 5 m (Figure 16 c). The agreement is good until 500 s. Then, the numerical simulation predicts temperature increase until the end whereas experimentally the smoke temperature rises slowly and drops at 700 s to 60 ºC, remaining constant. The largest differences are found at the end, when the relative error grows up to 65 %. This is due to the lowest parts are most sensitive to flow perturbations and they have not been simulated numerically. Good agreement is found between smoke layer height predictions and measurements.

The predicted smoke layer height has been compared with the experimental results using the N-percent method [29]. A temperature increase from ambient temperature of 10 – 20 % of the highest temperature rise has been typically been used to define the base of the transition zone between the smoke layer and the cold layer [29]. Other authors [14] locate the smoke layer where the temperature increase is of 30 % of the highest temperature rise in atria. In general, there is

good agreement between FDS predictions and the 30 % temperature increase. It is observed that the simulations slightly overestimate the final smoke layer height. This is in agreement with other works [14].

6.- Conclusions:

The paper presents the results from the three Murcia Fire Tests conducted in the large-scale atrium with heptane pools of two diameters. In two of the fire tests, Test 1 (1.32 MW) and Test 2 (2.28 MW), natural and mechanical ventilation have been combined. At Test 3 (2.34 MW), only natural ventilation has been used. The main objective was to provide a new complete set of experimental data for and to compare the results with modelling predictions.

Comparing of combined natural and forced ventilation (Tests 2) and only natural ventilation (Test 3) for the same fire size, it is observed that, for the particular case at hand, the use of mechanical exhaust leads to small differences in smoke temperature increase in the roof (19 % lower) or steady-state smoke height (7 % higher, respect total height), but leads to a 40 % reduction in velocity of the descending smoke layer to the lowest height.

CFD simulations using FDS4 have been conducted to check the code capability for predicting the fire-induced conditions in large enclosures. It has been observed that FDS4 simulations significantly over-predict by 40 to 80 % the plume temperature near the flame (below 9 m) but only slightly over-predict by 10 to 25 % the plume temperature above 9 m. These results agree well with those in the literature where the reported accuracy for high locations is between 5 to 20 % [22]. At the exhaust fans and the upper parts near the wall (above 10 m) the agreement is good too, and at lower part of the walls the predictions are poor, as with the plume. This has been also found in other works [21, 26]. For the design of smoke evacuation system, good predictions at higher locations are more important than prediction at lower heights. Thus, according to the results reported here, FDS could be a valid tool for performance-based design of smoke systems in large enclosures if properly used.

Acknowledgements:

The authors want to acknowledge the Centro Tecnológico del Metal of Murcia for the use of their test rig, the Professor J. L. Torero, T. Steinhaus, C.Abecassis-Empis, Dr P. Reszka, W. Jahn, from the University of Edinburgh, for their technical suggestions. Simulations have been carried out at the computational facilities of the Technological Research Services of the Technical University of Cartagena (SAIT) and the University of Jaen. This work has been supported by Ministerio de Educación y Ciencia of Spain (Projects CT/G30572473, and FIT-020700-2004-25 and grant TRA2006-15015) and by the Junta de Andalucía of Spain (Project number P07-TEP-02693). E.S.R. also acknowledges the “Ramón y Cajal” program by Ministerio de Educación y Ciencia of Spain.

References:

[1] Roaf, S., Crichton, D., Nicol, F. Adapting Buildings and Cities for Climate Change: A 21st Century Survival Guide (Chapter 2 – The Evolution of Buildings), Architectural Press – An imprint of Elsevier, Oxford (2005).

[2] G Rein, X Zhang, P Williams, B Hume, A Heise, A Jowsey, B Lane, JL Torero, "Multi-story Fire Analysis for High-Rise Buildings", Proceedings of the 11th International Interflam Conference, London, Sept. 2007. Copy available at http://hdl.handle.net/1842/1980

[3] NFPA 92B. Guide for smoke management systems in atria, covered malls, and large areas. Quincy, MA, USA: National Protection Association; 2005.

[4] Klote JH. New developments in atrium smoke management. ASHRAE Transactions 2000; 106, pp. 620–626.

[5] Ding, W., Minegishia, Y., Hasemib, Y., Yamada, T. Smoke control based on a solar-assisted natural ventilation system. Building and Environment, 2004, 39, pp. 775 – 782

[6] Quintiere, J.G. Scaling applications in fire research. Fire Safety Journal, 1989; 15, pp. 3-29.

[7] SFPE of Fire Protection of Engineering. 3rd ed. Quincy, MA, USA: National Fire Protection Association, 2002.

[8] Harrison, R. Smoke Control in Atrium Buildings: A Study of the Thermal Spill Plume, Fire Engineering Research Report 04/1, 2004, Christchurch, NZ: University of Canterbury.

[9] Qin, T.X., Guo, Y.C., Chan, C.K., Lin, W.Y. Numerical simulation of the spread of smoke in an atrium under fire scenario. Building and Environment, 2009, 44, pp. 56–65

[10] SFPE Engineering Guide to Performance-based Fire Protection. National Fire Protection Association (NFPA), Second Edition (January 31, 2007)

[11] Chow, W.K., Fong, N.K., Cui, E., Ho, P.L., Wong, T., Huo, R., Fan, W, Li, Y., Yuan, L. PolyU/USTC Atrium: A Full-Scale Burning Facility -- Preliminary Experiments. Journal of Applied Fire Science, 1999; 8(3).

[12] Chow WK, Li YZ, Cui E, Huo R. Natural smoke filling in atrium with liquid pool fires up to 1.6MW. Building and Environment, 2001; 36(1), pp.121–127.

[13] Yi L, Chow WK, Huo R, Fong NK, Li YZ, Leung CW, Shi CL, Hung WY, Wang HB. Full-scale burning tests on mechanical smoke exhaust in large atrium. ASHRAE Transaction 2004.

[14] Yi, L., Chow, W.K., Li, Y.Z., Huo, R. A simple two-layer zone model on mechanical exhaust in an atrium. Building and Environment, 2005; 40, pp. 869–880

[15] Shi, C.L, Lu, W.Z., Chow, W.K., Huo, R. An investigation on spill plume development and natural filling in large full-scale atrium under retail shop fire. International Journal of Heat and Mass Transfer, 2007, 50, pp. 513–529

[16] Hostikka, S., Kokkala, M. Vaari, J. Experimental study of the localized room fires.NFSC2 Test Series (VTT building technology) VTT Research Notes 2104. 2001

[17] Lougheed, G.D.; McCartney, C.J. Balcony spill plumes: full-scale experiments, Part 1. ASHRAE Transactions, v. 114, pt. 1, 2008, pp. 329-343.

[18] Gutiérrez-Montes, C., Sanmiguel-Rojas, E., S. Kaiser, A., Viedma, A. Numerical model and validation experiments of atrium enclosure fire in a new fire test facility. Building and Environment, 2008, 43 (11), pp: 1912–1928.

[19] Welch, S., Jowsey, A., Deeny, S., Morgan, R., Torero, J.L. BRE large compartment fire tests—Characterising post-flashover fires for model validation. Fire Safety Journal, 2007, 42, pp. 548–567.

[20] Tewarson, A. Combustion efficiency and its radiative component. Fire Safety Journal, 2004, 39, pp. 131-141.

[21] Dreisbach, J., McGrattan, K. Verification and Validation of Selected Fire Models for Nuclear Power Plant Applications, Volume 7: Fire Dynamics Simulator (FDS), NUREG-1824 Final Report, U.S. Nuclear Regulatory Commission, Office of Nuclear Regulatory Research, May 2007.

[22] McGrattan, K. Fire Dynamics Simulator (Version 4) Technical Reference Guide. Ed.,National Institute of Standards and Technology, Special Publication 1018, 2004.

[23] Pope, S.B. Computations of turbulent combustion: progress and challenges. Proceedings of the Combustion Institute, 1990, 23, pp. 591-612

[24] Hamins, A., Klassen, M., Gore, J. Kashiwagi, T. Estimate of Flame Radiance via single Location Measurement in Liquid Pool Fires Combustion and Flame, 86, 223-228, 1991.

[25] Incropera, F. P., DeWitt, D. P., Fundamentals of Heat and Mass Transfer. John Wiley & Sons; 4 Sub-edition , 1996

[26] Ma, T.G., Quintiere, J.G. Numerical simulation of axi-symmetric fire plumes: accuracy and limitations. Fire Safety Journal, 2003, 38; pp.467-492.

[27] McGrattan, K.B., Baum, H.R., Rehm, R.G. Large Eddy Simulations of Smoke Movement. Fire Safety Journal, 1998, 30, pp. 161-178.

[28] Heskestad, G. Engineering Relations for Fire Plumes. Fire Safety Journal, 1984, 7, pp. 25-32.

[29] Cooper, L.Y., Harkleroad, M., Quintiere, J., Reinkinen, W. An experimental study of upper hot layer stratification in full-scale multi-room fire scenarios. Journal of Heat and mass transfer, 1982; 104 pp. 741-749.